Journal of Physiology (1990), **428**, *pp.* 243–256
With 5 figures
Printed in Great Britain

RESTING CALCIUM CONCENTRATIONS IN ISOLATED SKELETAL MUSCLE FIBRES OF DYSTROPHIC MICE

BY DAVID A. WILLIAMS*, STEWART I. HEAD, ANTHONY J. BAKKER AND D. GEORGE STEPHENSON

*From the *Department of Physiology, University of Melbourne, Parkville, Victoria 3052 and the Department of Zoology, La Trobe University, Bundoora, Victoria 3083, Australia*

(*Received 8 January 1990*)

SUMMARY

1. Single, intact muscle fibres were dissociated enzymatically from skeletal muscles of phenotypically normal (+/?) and dystrophic mice (129/ReJ dy/dy; *Dystrophia muscularis*), and resting Ca^{2+} levels were measured by image analysis of intracellular Fura-2 fluorescence in distinct parts of the fibres.

2. Fura-2 was introduced into fibres by ionophoresis with glass microelectrodes to concentrations of between 50 and 200 μM. Over this concentration range there was no apparent buffering of intracellular Ca^{2+} by Fura-2.

3. Fibres isolated from the soleus, flexor digitorum brevis (FDB) and extensor digitorum longus (EDL) muscles of normal animals maintained resting [Ca^{2+}] of 106 ± 2 nM. Ca^{2+} distributions within individual fibres were homogeneous.

4. Fibres from dystrophic animals maintained [Ca^{2+}] that was elevated two- to fourfold in comparison to normal fibres.

5. The population of skeletal fibres from dystrophic mice which displayed morphology similar to that of fibres of normal animals were found to have Ca^{2+} levels that averaged 189 ± 2 nM. The distribution of Ca^{2+} within these fibres appeared uniform.

6. The population of dystrophic fibres that possessed morphological abnormalities maintained even higher Ca^{2+} concentrations (368 ± 3 nM). Several fibres from this morphological group displayed obvious heterogeneity in Ca^{2+} distribution with distinct, localized areas of higher Ca^{2+}.

7. These results support the contention that Ca^{2+} homeostasis is markedly impaired in dystrophic muscle. The elevated Ca^{2+} levels are near the threshold for contraction and, together with severe morphological fibre abnormalities, are probably centrally involved in fibre necrosis apparent in muscular dystrophy.

INTRODUCTION

The pathophysiology displayed in the autosomal murine model for muscular dystrophy 129/ReJ dy/dy shares a number of major characteristics with Duchenne muscular dystrophy (DMD), the most common human muscular dystrophy. The major characteristics include severe and progressive muscle weakness, progressive

degeneration of skeletal muscle, and elevated serum activity of myoplasmic enzymes (Rowland, 1985). In comparison, the dystrophy displayed by the X-chromosome-linked defect in the mdx mouse, although of similar origin to DMD (Hoffman, Monaco, Feener & Kunkel, 1987) shares very few of the clinical symptoms of DMD, and, unlike DMD individuals and the 129/ReJ model, these mice have a normal life expectancy (Brown & Hoffman, 1988). Therefore, we believe that the thorough investigation of the etiology of the dy/dy murine dystrophy will enhance our understanding of the degenerative and terminal stages of DMD.

Morphological abnormalities in the form of simple forks to complex branching structures have been recently described in the majority (up to 60%) of skeletal muscle fibres isolated from adult dystrophic mice 129/ReJ (dy/dy) (Head, Stephenson & Williams, 1990). No major differences were observed between the contractile properties of skinned fibre segments obtained from dystrophic fibres of normal appearance and from different regions of fibres with distinct morphological abnormalities. However, the presence of multiple branches and grooves may make these individual fibres susceptible to damage during the contraction of the intact muscle and, therefore, have major implications for muscle function in these dystrophic animals. These abnormalities may also contribute to a number of the symptoms which lead to the eventual death of the animal.

The primary motivation for the present study was to compare resting Ca^{2+} levels of single muscle fibres from skeletal muscle fibres of adult phenotypically normal (+/?) and dystrophic (129/ReJ, dy/dy) mice, because abnormalities in Ca^{2+} homeostasis have long been thought to be centrally involved in the dystrophic disease process (Bodensteiner & Engel, 1978; Duncan, 1978; Moser, 1984). It was also of interest to determine if the presence of morphological abnormalities within a fibre influenced Ca^{2+} homeostasis as we have previously shown this population to be prone to structural damage during contraction. Preliminary accounts of this work have previously appeared elsewhere in abstract form (Bakker, Head, Stephenson & Williams, 1989; Williams, Head, Bakker & Stephenson, 1989).

METHODS

Cell preparation and dye loading

Single, intact, skeletal muscle fibres were enzymatically isolated from three hindlimb muscles of both phenotypically normal (+/?) and dystrophic (dy/dy) mice (*Dystrophia muscularis*): extensor digitorum longus (EDL; predominantly fast twitch), flexor digitorum brevis (FDB; predominantly fast twitch) and soleus (mixed fast and slow twitch). Adult animals (10–14 weeks) were killed by overdose of diethyl ether prior to ablation of required muscles. The technique for fibre dissociation, which we have described in detail elsewhere (Head *et al.* 1990), was modified from that for intact rat muscle (Bekoff & Betz, 1977), and involved incubation of intact muscles in low-Ca^{2+} Tyrode solution with collagenase (type IV) at 35 °C for 2–3 h. In contrast to our previous study where the isolation method sometimes involved resuspension of dissociated fibres in an EGTA-containing relaxing solution (Head *et al.* 1989), in this study we always used fresh Tyrode solution containing 2 mM-Ca^{2+} to maintain membrane integrity and avoid fibre hyperpermeabilization. The resuspension of fibres in Ca^{2+}-containing media (Tyrode solution), reduced the yield of intact fibres from the digestion of both normal and dystrophic muscles. The procedure did not change the proportion of those fibres displaying morphological abnormalities.

Individual fibres were selected for ionophoresis if they twitched strongly when electrically stimulated. The membrane potential (V_m) was measured with an intracellular microelectrode filled with 3 M-KCl (20–30 MΩ). The data from fibres which had a V_m more positive than −60 mV were discarded. Cells were loaded with the fluorescent calcium indicator Fura-2 by ionophoresis of the

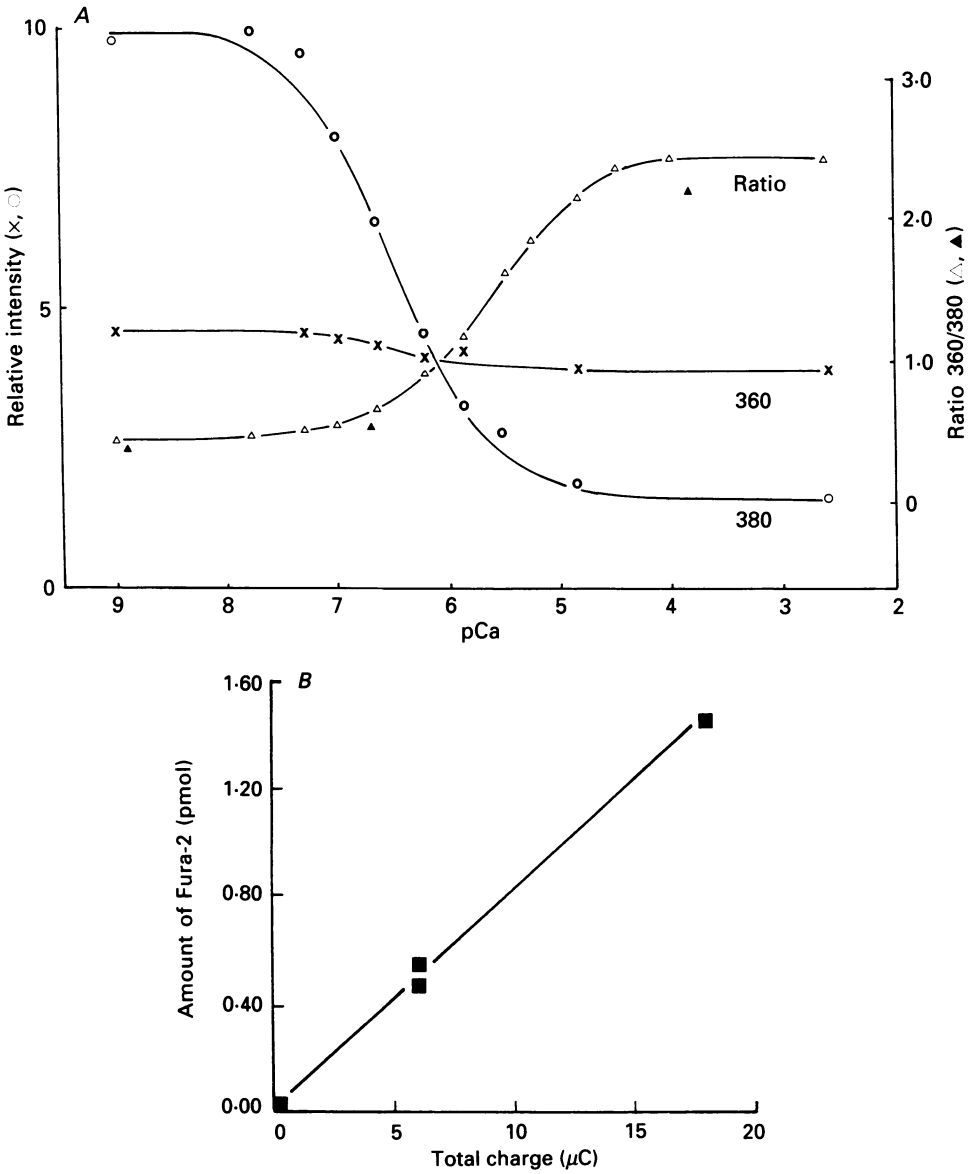

Fig. 1. *A*, calibration curve relating the ratio (△) of Fura-2 fluorescence emission excited at 360 and 380 nm to the [Ca^{2+}] of the calibrating solutions. The relative intensity levels recorded at 360 nm (×) and 380 nm (○) are also shown. [Ca^{2+}] was buffered with 10 mM-EGTA and free Ca^{2+} levels were determined by potentiometric titration (Stephenson & Williams, 1981). The calibrating solution also contained (mM): K^+, 100; Na^+, 30; Mg^{2+}, 1; HEPES, 10, pH 7·10. The ratio levels determined in three single fibres containing Fura-2 after treatment with Br-A23187 (10 μM) in otherwise identical calibrating solutions are also shown (▲). *B*, relation between amount of Fura-2 ionophoresed from a microelectrode into a solution bubble (see text) contained under paraffin oil, as a function of the total charge passed during 'test' ionophoresis periods. The amount of Fura-2 was derived from a calibration curve of fluorescence intensity for droplets of known volume and Fura-2 concentration. Total charge represents the product of current amplitude (nA) and total duration (s) of the test ionophoresis periods. Continuous lines representing theoretical curves for 1:1 binding of Ca^{2+} by Fura-2 (Hill relations for $n = 1$) were drawn through the experimental points. The ratio curve was obtained from experimental points (where available) or otherwise from these experimental curves.

penta-potassium salt (Molecular Probes, OR, USA) with a single fine-tipped microelectrode. Fura-2 (1 mM in distilled water) was introduced into the tapered tip of a microelectrode by capillary action down the thin central filament of the electrode. The shank of the electrode was then filled with 150 mM-potassium acetate solution. As Fura-2 is highly negatively charged (−5), passage of a negative current through the electrode expelled the dye into the impaled cell. An Axoclamp-2A was used in bridge mode so that the potential of the cell could be measured during ionophoresis. The pulse protocol for injection was controlled with a model D100 Digitimer that allowed for the delivery of a train of negative pulses of 6–10 nA amplitude of 1 s duration separated by 1 s pauses for a total period from 5 to 20 min. Fibres were then left for 30 min to allow for complete intracellular redistribution of Fura-2 before Ca^{2+} measurements commenced.

Image acquisition

The fluorescence of Fura-2-loaded skeletal muscle fibres was imaged with a Nikon CF-Fluor (×10, NA 0·5) or UV-F (×40, NA 1·30) objective and a Leitz inverted microscope equipped for xenon epifluorescence. Excitation wavelengths were alternated between 360 and 380 nm with an automated filter changer (Williams, Milhuisen, Kent, Hudson & Durham, 1988). This choice of wavelengths rather than the more commonly used values of 340 and 380 nm had the advantage of allowing for similar fluorescence transmissions in microscope optics resulting in similar signal-to-noise ratios in each wavelength image and only a small error in the calculated ratio image of resting cells (Moore, Becker, Fogarty, Williams & Fay, 1990). The major disadvantage was the reduction in the absolute dynamic range of the ratio measurement. As large dynamic changes in the $[Ca^{2+}]$ were not expected in the present study (e.g. fibres were not stimulated) reduction in the absolute range of the ratio was only a minor concern.

Video images were obtained with a silicon-intensified-target (SIT) camera with the camera output digitized to 8-bit resolution with an Imaging Technology (Dindima, Australia) FG-100-AT board resident in an Olivetti M-280 personal computer. Frame-averaged (eight frames) cellular and background (cell removed) images were obtained at both excitation wavelengths (360 and 380 nm). Spatial variations in dark current and excitation source intensity were corrected, and ratio (360/380) images were created by dividing background-corrected 360 and 380 nm images on a pixel-by-pixel basis as has been previously described (Williams, Fogarty, Tsien & Fay, 1985).

Image calibration and analysis

Ratio (360/380) images were analysed interactively by randomly selecting nine distinct sample areas throughout each fibre. Sample areas were chosen to be square to enhance reproducibility of the absolute area encompassed within each box. Each box represented an area from 25 to 225 μm^2 (depending on image magnification) of the cell cytoplasm. Areas were chosen to exclude fibre edges where low signal-to-noise ratios in the individual single-wavelength images introduced large errors into the calculation of $[Ca^{2+}]$. The ratio value for each individual sample area was converted to Ca^{2+} (as described below) and the mean and S.E.M. of the nine Ca^{2+} values was calculated for each fibre. Ca^{2+} concentrations within an individual fibre were classified as being homogenously distributed if the standard deviation of the mean fibre $[Ca^{2+}]$ was less than 5%.

Ratio values were calibrated in terms of actual Ca^{2+} concentration by experimentally determining fluorescence constants (R_{min}, R_{max}, β) and the apparent dissociation constant (K_d) of Fura-2 for Ca^{2+} (Grynkeiwicz, Poenie & Tsien, 1985). The K_d was calculated for our experimental conditions by constructing a series of strongly buffered Ca^{2+}-containing solutions by varying the ratio of CaEGTA to EGTA in each solution. The CaEGTA/EGTA ratio was precisely determined by potentiometric techniques developed in this laboratory (Stephenson & Williams, 1981). These solutions were used to determine the *in vitro* relation between fluorescence intensity of Fura-2 (360 and 380 nm excitation, 500 nm emission) and the actual $[Ca^{2+}]$ of the calibration solution. This relationship is illustrated in Fig. 1*A*. A similar protocol was applied to three individual, Fura-2-loaded muscle fibres treated with the ionophore Br-A23187 under conditions of saturating (pCa 4·5) and zero (pCa > 8·5) calcium, and at a $[Ca^{2+}]$ which approximated the K_d for Ca-Fura-2 (pCa ~ 6·7). These *in vivo* values are also included in Fig. 1*A*. It is clear that at all three Ca^{2+} levels the ratio measured in loaded cells differed from that for the free cation Fura-2 in calibrating solutions by approximately 12%. Therefore, to correct for this discrepancy, *in vitro* values for R_{max} and R_{min} were reduced by 12% before deriving $[Ca^{2+}]$ from Fura-2-loaded muscle fibres, a similar correction to that recently described for smooth muscle (Moore *et al.* 1990). The effective K_d used in these

experiments for Ca^{2+} determinations was 298 nM. Hill plots of the single-wavelength fluorescence (360 or 380 nM) and pCa (not shown), supported the 1:1 binding of Ca^{2+} by Fura-2 in our experimental system. The calibration techniques have recently been described in detail (Williams & Fay, 1990).

Internal dye concentrations

Intracellular dye concentrations were estimated in each experiment with one of two distinct protocols. In several experiments a similar method to that described by Moore *et al.* (1990) for smooth muscle cells was used. Briefly, absolute fluorescence intensities of discrete cellular areas recorded at 360 nm were compared with the absolute fluorescence intensities at the same wavelength of a droplet of Fura-2 acid contained within water-saturated Zeiss immersion oil. The volume of the Fura-2 droplet and the muscle fibre loaded with Fura-2 were estimated from diameter measurements assuming spherical and cylindrical profiles respectively.

Intracellular dye concentrations were also directly calculated from the ionophoresis parameters (pulse amplitude and duration) and the estimated volume of the injected cell. The concentration of Fura-2 ionophoresed into a known volume of a solution mimicking the intracellular environment (type A pCa > 8, see Stephenson & Williams, 1981) was first determined using a fluorescence calibration curve obtained with known Fura-2 concentrations. The amount of Fura-2 ionophoresed (concentration × volume of droplet) was then expressed as a function of the total charge (current amplitude × duration) passed through the electrode during ionophoresis. This experimental relation is illustrated in Fig. 1*B* and indicates a linear dependence of amount of Fura-2 on charge passed. Intracellular [Fura-2] could be directly calculated from the total charge passed and estimated volume of each fibre. In the individual fibres used in these experiments [Fura-2] was calculated to be in the range 50–250 μM with both methods.

RESULTS

Calcium in single muscle fibres from normal animals

A ratio (360/380) image of a Fura-2-loaded, single muscle fibre from the FDB (flexor digitorum brevis) of a phenotypically normal mouse is shown in Fig. 2. This fibre is an elongated, unbranched structure as we have previously described for enzymatically dispersed, skeletal muscle fibres of normal animals. As is typical for muscle fibres from the mouse FDB this fibre is short (0·7 mm in length) with an average diameter of 30 μm. The intensity ratios of all sample areas analysed within the fibre were almost identical and equated to a homogeneously distributed, average intracellular [Ca^{2+}] of 124 ± 2 nM (mean ± S.E.M.). Measurements of [Ca^{2+}] made in fibres enzymatically dissociated from the other muscles (soleus and EDL) of phenotypically normal (+/?) mice showed similar resting levels (106 ± 2 nM; see Table 1).

The ionophoresis procedure used in this study for loading single skeletal fibres with the Ca^{2+}-sensitive fluorescent indicator allowed for control over the actual concentration of Fura-2 internalized. This control was used to investigate the potential buffering of these intracellular Ca^{2+} levels by the intracellular concentrations of Fura-2 introduced into fibres. A single soleus fibre from a phenotypically normal (+/?) animal was ionophoresed for a 5 min period, after which the average fibre calcium concentration was determined to be 98 ± 3 nM for nine sample areas (see Methods). The microelectrode was then reinserted to continue the ionophoresis procedure. After a further 10 min filling period the electrode was again removed and average [Ca^{2+}] in the fibre was redetermined. Fura-2 concentrations were estimated from the ionophoresis parameters (as described in Methods; see Fig. 1*B*), and were found to increase by a factor of 4 following the initial

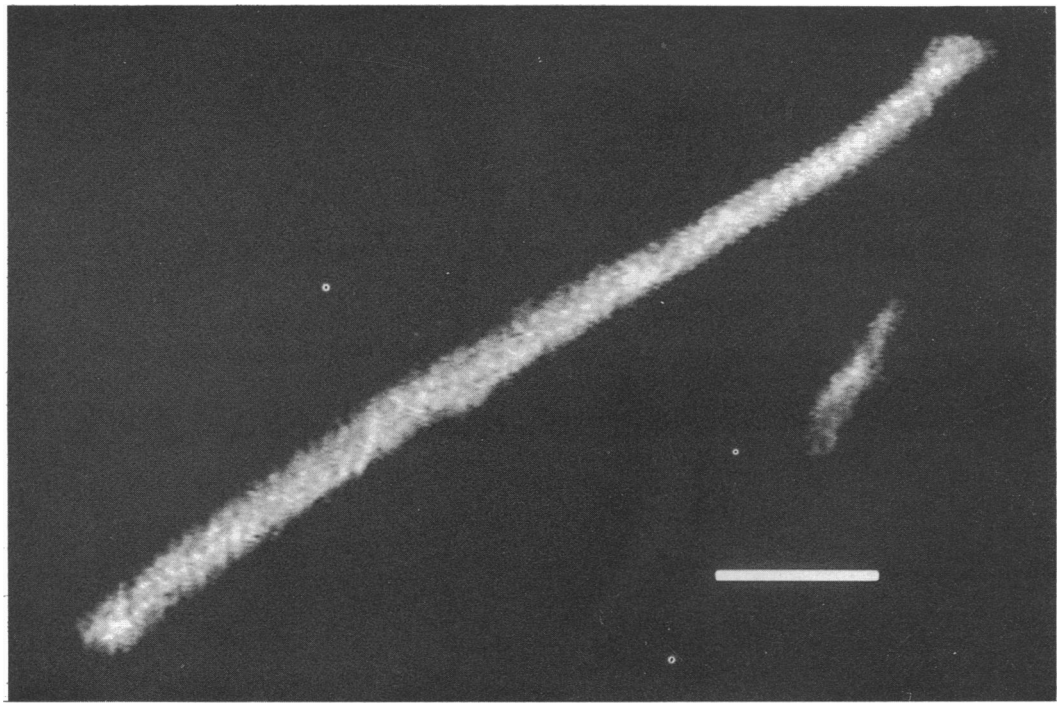

Fig. 2. Image of the ratio of fluorescence intensity of Fura-2 excited at 360 and 380 nm for a single fibre from the FDB of a phenotypically normal (+/?) mouse. Ionophoresis parameters: pulse amplitude −8 nA, total duration of 180 s. Intracellular [Fura-2] was calculated (from Fig. 1*B*) to be 234 μM. Scale bar, 100 μm.

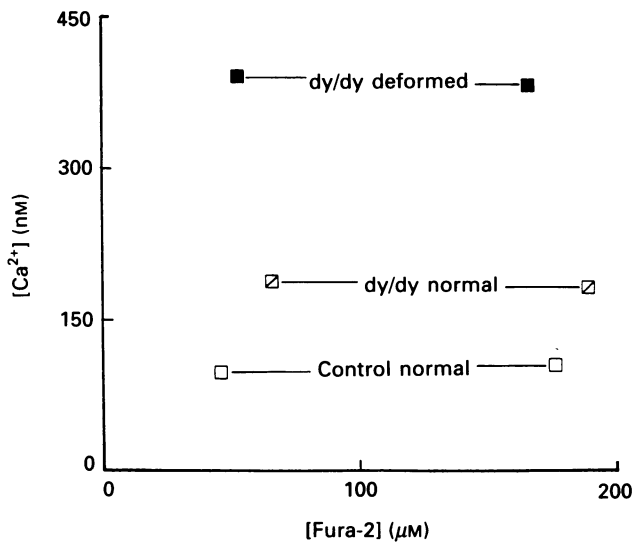

Fig. 3. The effects of intracellular [Fura-2] on the resting [Ca^{2+}] of an individual soleus fibre of a phenotypically normal (+/?) mouse (□), and a morphologically normal (▨), and a deformed soleus (■) fibre from a dystrophic (dy/dy) mouse. Fura-2 concentrations were estimated from the ionophoresis parameters used to introduce the dye into each fibre, while average [Ca^{2+}] levels were determined with the image calibration procedure, both described in the Methods section. The standard error of each Ca^{2+} estimation lies within the boundaries of each symbol.

period of ionophoresis to a final concentration of 150–190 μM. This increase in Fura-2 had no apparent effect on the resting Ca^{2+} level in this fibre which was now estimated to be 105 ± 1 nM for the same sample areas. This result is presented diagrammatically in Fig. 3 and strongly suggests that the range of Fura-2 concentrations which were used in these experiments (50–250 μM) did not affect

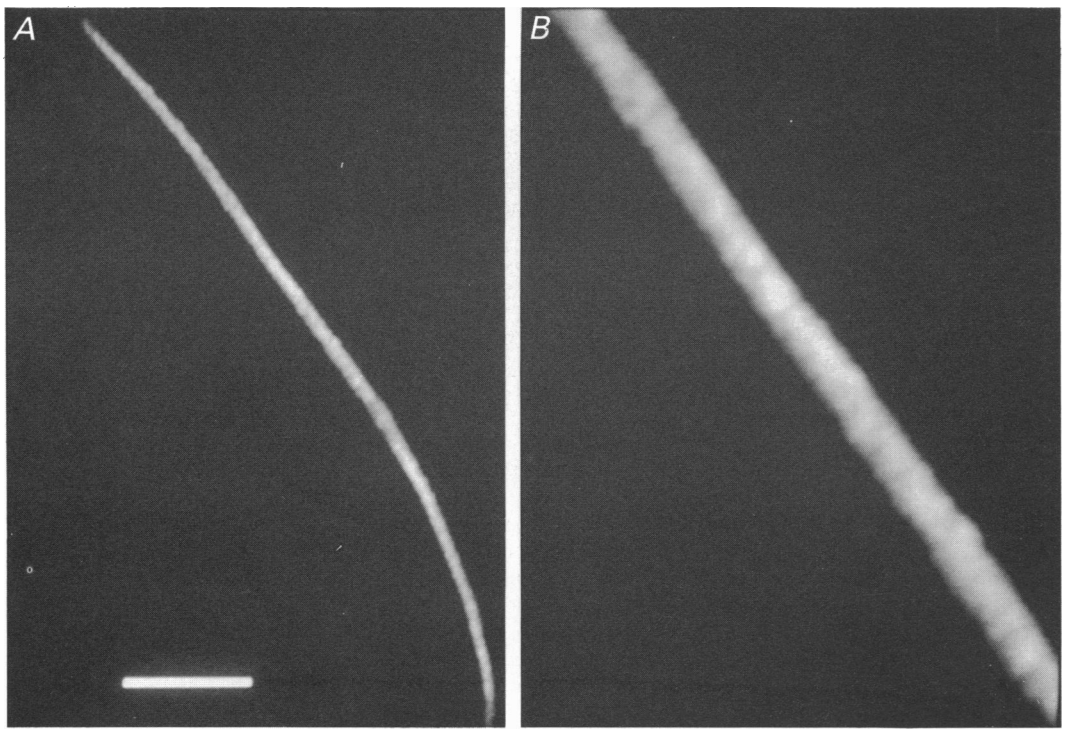

Fig. 4. *A*, ratio (360/380 nm) image of Fura-2 fluorescence for a morphologically normal EDL muscle fibre of a dystrophic (dy/dy) mouse. *B*, ratio image of a section of the same fibre captured with a higher magnification and higher numerical aperture objective (Nikon CF UV-F ×40, NA 1·30). Ionophoresis parameters: pulse amplitude −6 nA, total duration 360 s. Intracellular [Fura-2], 135 μM. Scale bar: *A*, 250 μm; *B*, 100 μm.

resting $[Ca^{2+}]$. Moreover, these results also show that electrode insertion for the ionophoresis procedure did not itself markedly damage the cell membrane as there was no irreversible increase in intracellular $[Ca^{2+}]$ following the second (or subsequent) fibre penetration.

Calcium in single fibres of dystrophic animals

Fibres isolated from the soleus and EDL muscles of adult dystrophic mice (dy/dy) could be separated into two major groups based solely on morphological criteria as we have previously described. Some fibres (30–40 %) showed a similar, unbranched, elongated morphology to that of fibres from phenotypically normal (dy/dy) mice. A ratio image (360/380 nm) of one such EDL fibre is displayed in Fig. 4*A*. Ratio values calculated for the sample areas of this fibre showed little variability, again indicative

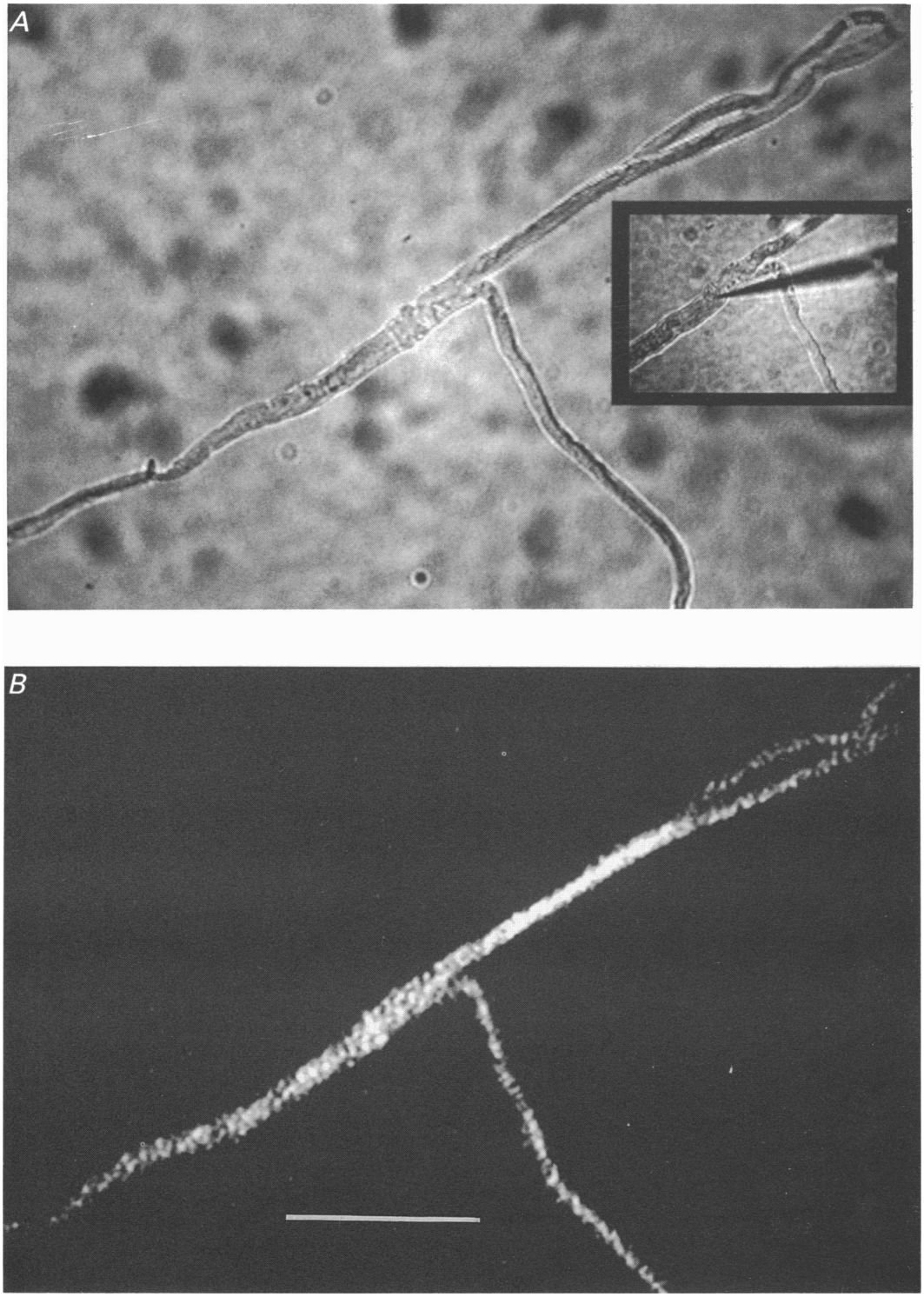

Fig. 5*A* and *B*. For legend see facing page.

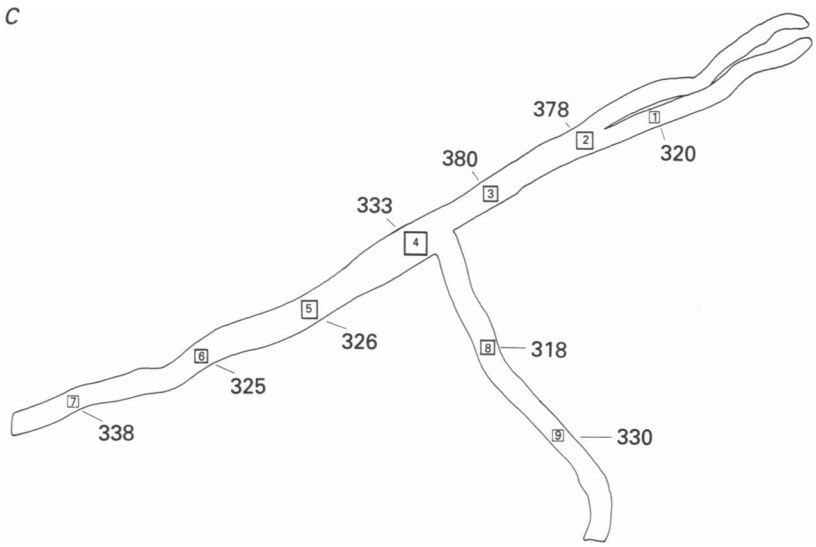

Fig. 5. *A*, bright-field image of a single morphologically abnormal fibre from the soleus muscle of a dystrophic mouse (dy/dy). The inset shows the point of insertion of the ionophoresis electrode under higher magnification. *B*, fluorescence ratio (360/380) image for the same malformed single fibre. Contrast scaling was chosen to highlight the small diversity of Ca^{2+} levels within discrete regions of the fibre. *C*, diagram indicating the position and $[Ca^{2+}]$ (nM) of sample areas chosen in this fibre. The distal parts of the smallest calibre branched sections of the fibre were generally not designated as sample areas because of low absolute signal-to-noise ratios in the individual wavelength images. Individual pixels were omitted from $[Ca^{2+}]$ calculations if their fluorescence intensity was not significantly (greater that 3 image standard deviations) above background intensity level. Ionophoresis parameters: pulse amplitude −9 nA, total duration 400 s. Intracellular [Fura-2], 167 μM. Scale bar, 250 μm.

of a relatively homogeneous distribution of $[Ca^{2+}]$ within the fibre. Even when images were obtained for the same fibre with higher magnification and higher numerical aperture objectives (Fig. 4*B*; ×40, NA 1·30), there were no apparent inter- or intrasarcomere differences in Ca^{2+} levels. However, the average resting Ca^{2+} concentration of this fibre, 204±2 nM, and other fibres from this morphological group of dystrophic fibres (average 189±2 nM; Table 1), was significantly higher ($P < 0{\cdot}001$, *t* test) than for fibres of similar morphology from phenotypically normal (+/?) mice (see Table 1).

In contrast, a large percentage (60%) of muscle fibres from dystrophic mice (dy/dy) displayed branched morphologies ranging from the presence of minor processes to complex associations of multiple fibre sections. The single soleus muscle fibre displayed in Fig. 5*A* is characteristic of the types of morphological abnormalities we have previously described in this population of dystrophic fibres (Head *et al.* 1990). This fibre has three major branches radiating from the main fibre axis. The fluorescence ratio (360/380) image of this fibre is shown in Fig. 5*B* and indicates that Fura-2 has been able to enter all branches from the point of entry of the ionophoresing electrode (shown in Fig. 5*A*, inset). This observation re-emphasizes

that this complex syncytium represents a functional single muscle fibre as we have previously shown. In contrast to the apparent [Ca^{2+}] homogeneity within individual fibres of normal morphology (Figs 2 and 4), there was a marked variation in the calculated ratios for the individual sample areas of the morphologically abnormal dystrophic soleus fibre. The location of the nine sample areas and the Ca^{2+} levels determined for these areas are diagrammatically shown in Fig. 5*C* (see also Table 1). [Ca^{2+}] ranged from 318 to 380 nM within these areas. However, it is interesting to note that the [Ca^{2+}] determined within the two branches included in the measurements (areas 1, 8 and 9) exhibited similar values to those found within most sample areas of the main fibre body (areas 4–7). The marked diversity of [Ca^{2+}] (also reflected in a relatively large S.E.M.; see Table 1), can be largely attributed to the higher Ca^{2+} values determined within areas 2 and 3 of the main fibre body. Resting Ca^{2+} levels averaged 339 ± 8 nM ($n = 9$ sample areas) throughout the main fibre body and major fibre appendages. One other soleus fibre of the seven total malformed fibres of dystrophic muscle used in this investigation also displayed a large variation in resting Ca^{2+} level as reflected in the higher standard error (see Table 1), and this could also be attributed to several distinct areas of high ratio intensity within the fibre (image not shown).

The potential contribution of introduced Fura-2 to Ca^{2+}-buffering capacity was also determined for dystrophic fibres. A fibre from each morphological group was used and these results are also presented graphically in Fig. 3. In the dystrophic soleus fibre of normal morphology [Ca^{2+}] was estimated as 188 ± 6 and 182 ± 8 nM after the first and subsequent ionophoresis period, respectively. Similarly, estimated [Ca^{2+}] was unaffected by the second ionophoresis period (382 ± 8 nM compared to 390 ± 6 nM) in a malformed soleus fibre from dystrophic muscle. In these fibres there was no significant difference ($P > 0{\cdot}1$, *t* test) between averaged intracellular [Ca^{2+}] calculated after the initial and subsequent ionophoresis periods.

Average intracellular Ca^{2+} levels recorded in all individual fibres used in this study are summarized in Table 1. Within a given morphological group there were no major differences in Ca^{2+} levels between fibres from each muscle type (EDL, FDB or soleus). Single fibres from phenotypically normal (+/?) mice maintained significantly lower average resting Ca^{2+} levels (106 ± 2 nM; mean $\pm$ S.E.M.), than either morphologically normal or deformed fibres from dystrophic (dy/dy) mice. The [Ca^{2+}] of the two morphologically distinct populations of muscle fibres from dystrophic animals (normal and deformed) also differed significantly ($P < 0{\cdot}05$) from each other, with resting levels of 189 ± 2 and 368 ± 3 nM, respectively, although there was no significant difference between [Ca^{2+}] of EDL and soleus fibres within the malformed dystrophic fibre population.

DISCUSSION

Fura-2 has been widely used to measure the concentration of free Ca^{2+} ions in the cytoplasm of different mammalian and amphibian isolated cells. Its use with striated muscle, and in particular with skeletal muscle, has been more restricted because of potential dye signal saturation at elevated (stimulated) Ca^{2+} levels. There have also been recent reports of possible interaction of Fura-2 with immobile structures such as contractile filaments in amphibian skeletal muscle (Baylor & Hollingworth, 1988).

However, in the present study the difference between intracellular and *in vitro* calibration parameters was of the same magnitude (12%) as that described for other cell systems (Poenie, Alderton, Steinhardt & Tsien, 1986; Moore *et al.* 1990), where Fura-2 binding to intracellular elements such as fixed contractile filaments would be minimal. This indicator should, therefore, be ideally suited to investigation of resting Ca^{2+} distribution in isolated mammalian skeletal muscle systems.

TABLE 1. Ionized calcium concentrations measured in individual muscle fibres

Animal	Fibre morphology	Muscle type	Sarcomere length* (μm)	$[Ca^{2+}]$ ($x \pm$ S.E.M.) (nM)
Control	Normal	EDL	2·6	87 ± 2 ($n = 9$)
Control	Normal	FDB	2·5	124 ± 2^{a} ($n = 9$)
Control	Normal	FDB	2·6	109 ± 2 ($n = 9$)
Control	Normal	Soleus	2·8	105 ± 1 ($n = 9$)
Mean: 106 ± 2 ($n = 36$) (range: 79–133)				
dy/dy	Normal	EDL	2·4	204 ± 2^{b} ($n = 9$)
dy/dy	Normal	EDL	2·6	182 ± 2 ($n = 9$)
dy/dy	Normal	Soleus	2·8	182 ± 3 ($n = 9$)
Mean: 189 ± 2 ($n = 27$) (range: 174–214)				
dy/dy	Deformed	EDL	2·7	382 ± 4 ($n = 9$)
dy/dy	Deformed	EDL	2·6	335 ± 3 ($n = 9$)
dy/dy	Deformed	EDL	2·7	368 ± 5 ($n = 9$)
dy/dy	Deformed	EDL	2·9	373 ± 4 ($n = 9$)
dy/dy	Deformed	Soleus	2·6	339 ± 8^{c} ($n = 9$)
dy/dy	Deformed	Soleus	2·9	382 ± 3 ($n = 9$)
dy/dy	Deformed	Soleus	2·7	400 ± 8 ($n = 9$)
Mean: 368 ± 3 ($n = 63$) (range: 318–433)				

n = number of sample areas. Group means were calculated for all sample areas used for each fibre in a group.

* Sarcomere lengths were estimated from bright-field video images of each fibre recorded after ionophoresis.

The superscripts a, b and c indicate the individual fibres displayed in Figs 2, 4 and 5 respectively.

Resting levels determined with Fura-2 in single fibres from phenotypically normal (+/?) mice averaged 106 ± 2 nM. A number of previous investigations in normal skeletal muscle, utilizing either Ca^{2+}-selective microelectrodes (Lopez, Alamo, Caputo, Wikinski & Ledezma, 1985; Sanchez, Bhattacharaya, Lopez, Sreter & Vergara, 1987), alternative fluorescent Ca^{2+} indicators (Mongini, Ghigo, Doriguzzi, Bussolino, Pescarmona, Pollo, Schiffler & Bosia, 1988), or loading with esterified forms of Fura-2 (Iaizzo, Seewald, Oakes & Lehmann-Horn, 1989), and in which the muscle preparations were derived from biopsy samples or cells in culture, have reported values for resting $[Ca^{2+}]$ comparable to that of the present study. This presents important support for the accuracy and suitability of measurements of Ca^{2+} levels made with different techniques in skeletal muscle. It also suggests that the enzymatic dissociation process, which involved exposure of muscles to collagenase activity exclusively, had not itself affected the structural integrity of muscle fibre membranes.

In addition this similarity verifies that the enzymatically isolated skeletal muscle fibre (Bekoff & Betz, 1977; Head *et al.* 1990) is a valuable preparation for measurements of both contractile parameters and ionic distributions.

Single skeletal muscle fibres from dystrophic (129/ReJ, dy/dy) mice maintained significantly higher (2- to 4-fold) resting calcium concentrations than fibres from phenotypically normal (+/?) mice. This is not unexpected given the previous reports of abnormal calcium homeostasis involved in the etiology of muscular dystrophy (Moser, 1984). What is more remarkable is the maintenance of significantly different resting Ca^{2+} levels by the two morphologically distinct fibre pools from the skeletal muscles of dystrophic mice. Ca^{2+} levels are 2-fold higher in the malformed fibre population than in dystrophic fibres which display normal morphology. This represents the first report of such discrete populations of muscle fibres with distinctly different Ca^{2+} levels within a diseased muscle fibre population.

There are many potential mechanisms for the maintained [Ca^{2+}] difference between skeletal muscle fibres from normal and dystrophic mice but presumably the causal process involves a change in the balance between the Ca^{2+} influx and Ca^{2+} extrusion processes involved in normal cellular Ca^{2+} homeostasis. If the membrane (sarcolemmal and/or sarcoplasmic reticulum) properties and/or integrity are affected in this murine dystrophy then we might expect that the Ca^{2+} homeostatic mechanisms in affected fibres would also be modified. In support of this contention are the reports of reduced microsomal levels of CaATPase activity in skeletal muscles of animals with either the same autosomal chromosome-linked dystrophy (129/ReJ, dy/dy), or a related dystrophy (dy^{2J}/dy^{2J}) (Lucas-Heron, Loirat, Ollivier & Leoty, 1987; Leberer, Hartner & Pette, 1988). In tandem with possible decreases in the structural integrity of the plasmalemma, which would lead to increased passive Ca^{2+} influx, these processes have the potential to equate to progressive long term elevation in cytosolic Ca^{2+} levels. A number of previous reports of elevated [Ca^{2+}] in skeletal muscle of other disease pathologies which are also thought to be linked to a membrane-associated lesion further support this point of view. Some of these include human muscular dystrophy (Mongini *et al.* 1988), and muscular dystrophy in *mdx* mice (Turner, Westwood, Regen & Steinhardt, 1988) and in hamsters (Sanchez *et al.* 1987).

The presence of a subpopulation of fibres (morphologically normal), within the dystrophic fibre population, that maintain Ca^{2+} levels between those of normal muscle and the malformed dystrophic population is interesting. It may suggest that the mechanistic cause of the elevation of resting Ca^{2+} levels is a progressive process and that this population represents an intermediate stage in a progressive Ca^{2+} elevation. This is further supported by the decline in the proportion of this morphologically normal fibre population in older (20 weeks) dystrophic animals (D. A. Williams, S. I. Head, A. J. Bakker & D. G. Stephenson, unpublished observations).

The elevated resting Ca^{2+} levels (368 ± 2 nM) maintained by the malformed population of skeletal fibres from 129/ReJ dy/dy mice are just below the [Ca^{2+}] which represents the contraction threshold for skeletal muscle fibres of the dystrophic (Head *et al.* 1990) and *mdx* (D. A. Williams, S. I. Head, G. S. Lynch & D. G. Stephenson, unpublished observations) murine dystrophies. Further progression of

the elevations of cytosolic Ca^{2+} levels would lead to fibres exceeding the contraction threshold and undergoing perpetual submaximal fibre contraction resulting in eventual fibre necrosis. This may explain why fibres with higher Ca^{2+} levels were not encountered in this and other studies of Ca^{2+} levels in muscle disease.

Beside the classical symptoms of progressive muscle necrosis and elevated serum levels of myoplasmic enzymes (Rowland, 1985), we have shown that mice with the autosomal chromosome-linked dystrophy (129/ReJ, dy/dy) possess morphological abnormalities (Head *et al.* 1990) and elevated myoplasmic [Ca^{2+}] (this study). These features are also apparent in individuals with DMD (Isaacs, Bradley & Henderson, 1973; Mongini *et al.* 1988), and this underlines the remarkable similarity between the end-stage etiology of this murine dystrophy and that exhibited in DMD.

We acknowledge the expert technical assistance of R. I. Cafarella and thank Dr G. D. Lamb for useful discussions. Supported by the National Health and Medical Research Council (NH&MRC) of Australia.

REFERENCES

BAKKER, A. J., HEAD, S. I., STEPHENSON D. G. & WILLIAMS, D. A. (1989). Calcium levels in skeletal muscle fibres from phenotypically normal and dystrophic mice (129/ReJ +/?, dy/dy). *Journal of Physiology* **412**, 51*P*.

BAYLOR, S. M. & HOLLINGWORTH, S. (1988). Fura-2 calcium transients in frog skeletal muscle fibres. *Journal of Physiology* **403**, 151–192.

BEKOFF, A. & BETZ, W. (1977). Physiological properties of dissociated muscle fibres obtained from innervated and denervated adult rat muscle. *Journal of Physiology* **271**, 25–40.

BODENSTEINER, J. B. & ENGEL, A. G. (1978). Intracellular calcium accumulation in Duchenne dystrophy and other myopathies: A study of 567,000 muscle fibers in 114 biopsies. *Neurology* **28**, 439–445.

BROWN, R. H. & HOFFMAN, E. P. (1988). Molecular biology of Duchenne muscular dystrophy. *Trends in Neurosciences* **11**, 480–484.

DUNCAN, C. J. (1978). Role of intracellular calcium in promoting muscle damage: a strategy for controlling the dystrophic condition. *Experientia* **34**, 1531–1535.

GRYNKIEWICZ, G., POENIE, M. & TSIEN, R. Y. (1985). A new generation of Ca^{2+} indicators with greatly improved fluorescence properties. *Journal of Biological Chemistry* **260**, 3440–3450.

HEAD, S. I., STEPHENSON, D. G. & WILLIAMS, D. A. (1990). Properties of enzymatically isolated skeletal fibres from mice with muscular dystrophy. *Journal of Physiology* **422**, 351–367.

HOFFMAN, E. P., MONACO, A. P., FEENER, C. C. & KUNKEL, L. M. (1987). Conservation of the Duchenne muscular dystrophy gene in mice and humans. *Science* **238**, 347–350.

IAIZZO, P. A., SEEWALD, M., OAKES, S. G. & LEHMANN-HORN, F. (1989). The use of fura-2 to estimate myoplasmic [Ca^{2+}] in human skeletal muscle. *Cell Calcium* **10**, 151–158.

ISAACS, D. R., BRADLEY, W. G. & HENDERSON, G. (1973). Longitudinal fibre splitting in muscular dystrophy: a serial cinematographic study. *Journal of Neurology, Neurosurgery and Psychiatry* **36**, 813–819.

LEBERER, E., HARTNER, K. & PETTE, D. (1988). Postnatal development of Ca^{2+}-sequestration by the sarcoplasmic reticulum of fast and slow muscles in normal and dystrophic mice. *European Journal of Biochemistry* **174**, 247–253.

LOPEZ, J. R., ALAMO, L., CAPUTO, C., WIKINSKI, J. & LEDEZMA, D. (1985). Intracellular ionized calcium concentration in muscle from humans with malignant hyperthermia. *Muscle and Nerve* **8**, 355–358.

LUCAS-HORN, B., LOIRAT, M. J., OLLIVIER, B. & LEOTY, C. (1987). Calcium-related defects in cardiac and skeletal muscles of dystrophic mice. *Comparative Biochemistry and Physiology* **86**, 295–301.

MONGINI, T., GHIGO, D., DORIGUZZI, C., BUSSOLINO, F., PESCARMONA, G., POLLO, B., SCHIFFLER, D. & BOSIA, A. (1988). Free cytoplasmic Ca^{2+} at rest and after cholinergic stimulus is increased in cultured muscle cells from Duchenne muscular dystrophy patients. *Neurology* **38**, 476–480.

MOORE, E. D. W., BECKER, P. L., FOGARTY, K. E., WILLIAMS, D. A. & FAY, F. S. (1990). Ca^{2+} imaging in single living cells: theoretical and practical issues. *Cell Calcium* **11**, 157–179.

MOSER, H. (1984). Duchenne muscular dystrophy: pathogenetic aspects and genetic prevention. *Human Genetics* **66**, 17–40.

POENIE, M., ALDERTON, J., STEINHARDT, R. & TSIEN, R. Y. (1986). Calcium rises abruptly and briefly throughout the cell at the onset of anaphase. *Science* **233**, 886–889.

ROWLAND, L. P. (1985). Clinical perspective: phenotypic expression in muscular dystrophy. *Advances in Experimental and Medical Biology* **182**, 3–13.

SANCHEZ, V., BHATTACHARYA, S., LOPEZ, J. R., SRETER, F. & VERGARA, J. (1987). Myoplasmic Ca^{2+} concentration in dystrophic hamsters. *Biophysical Journal* **51**, 551a.

STEPHENSON, D. G. & WILLIAMS, D. A. (1981). Calcium-activated force responses in fast- and slow-twitch skinned muscle fibres of the rat at different temperatures. *Journal of Physiology* **317**, 281–302.

TURNER, P. R., WESTWOOD, T., REGEN, C. M. & STEINHARDT, R. A. (1988). Increased protein degradation results from elevated free calcium levels found in muscle from *mdx* mice. *Nature* **335**, 735–738.

WILLIAMS, D. A. & FAY, F. S. (1990). Intracellular calibration of the fluorescent calcium indicator fura-2. *Cell Calcium* **11**, 75–83.

WILLIAMS, D. A., FOGARTY, K. E., TSIEN, R. Y. & FAY, F. S. (1985). Calcium gradients in single smooth muscles cells revealed by the digital imaging microscope using Fura-2. *Nature* **318**, 558–561.

WILLIAMS, D. A., HEAD, S. I., BAKKER, A. J. & STEPHENSON, D. G. (1989). Calcium imaging in normal and dystrophic skeletal muscle fibres. *Proceedings of the Australian Physiological and Pharmacological Society* **20**, 48A.

WILLIAMS, D. A., MILHUISEN, C., KENT, M., HUDSON, I. & DURHAM, L. (1988). Versatile multi-wavelength apparatus for cellular fluorescence microscopy. *Proceedings of the Australian Physiological and Pharmacological Society* **19**, 70*P*.